# Indium-doped GaAs: A very dilute alloy system

J. P. Laurenti,* P. Roentgen, K. Wolter, K. Seibert, and H. Kurz
*Institute of Semiconductor Electronics, Aachen Technical University, D-5100 Aachen, Federal Republic of Germany*

J. Camassel
*Groupe d'Etude des Semiconducteurs, Université des Sciences et Techniques du Languedoc, F-34060 Montpellier Cédex, France*

(Received 3 August 1987)

The influence of indium incorporation in GaAs organometallic–vapor-phase-epitaxy (OMVPE) layers has been investigated in great detail. The results obtained concern the change in band-gap energy, the concentration of residual impurities, and the low-temperature (2-K) photoluminescence (PL) efficiency. For In concentrations ranging between 0 and $6.5\times10^{19}$ cm$^{-3}$, both $A^0X$ and $D^0X$ bound-exciton lines could be resolved. Together with the near-band-gap transitions involving shallow impurities ($DA$- and $eA$-related recombination lines), they shift toward lower energies versus indium content. This indicates the formation of a ternary compound $Ga_{1-x}In_xAs$, even at these extremely dilute indium concentrations. After a quantitative calibration of the indium content, linear relations have been found which connect the PL emission line energies and the indium concentration. They make low-temperature PL measurements the most quantitative, and nondestructive, tool for precise composition studies. In this case, care should be taken that the slope parameters are line dependent. For instance, we find a slight, but finite, discrepancy between the slope parameters corresponding to substitutional acceptors on Ga and As sites, respectively. This is discussed in terms of the two different sublattices by using a simple cluster model of 17 atoms. Lastly, we find the absolute PL intensities to increase versus indium concentration: This indicates an improvement in the optical quality of our samples. Since, on a relative scale, the PL signals involving $Zn_{Ga}$ and/or $Mg_{Ga}$ residual acceptors are not significantly affected by the amount of indium incorporated, but depend mainly on the growth sequence, we feel that indium in GaAs acts primarily by closing nonradiative-recombination paths which are not necessarily associated with gallium vacancies.

## I. INTRODUCTION

During the growth of bulk GaAs crystals, a noted reduction of dislocation density has been obtained by incorporating indium.[1] Consequently a significant improvement of electrical substrate properties has been achieved which stimulated considerable interest in the field of semiconductor technology.[2] This method of indium incorporation has been extended to GaAs epitaxial layers and, in some cases, a strong reduction of deep centers concentration has been claimed[3] in comparison to conventional epilayers. This seems to correlate with significant improvements in device characteristics.[4,5]

To clarify the actual role of indium, a systematic study of defect centers at different calibrated indium concentrations is necessary. In the first step, the behavior of the band-gap energy, bound-exciton lines, and shallow level defects should be investigated. Very few works along this path can be found in the recent literature. First Kitahara *et al.*[6] analyzed the shift of the main luminescence lines for bulk semi-insulating (s.i.) GaAs:In crystals, with indium concentrations ranging between 1 and $3\times10^{20}$ cm$^{-3}$. More recently Yu *et al.*[7] repeated the same experiments in the range $(0.5-1.8)\times10^{20}$ cm$^{-3}$. They both worked on single crystals grown by the liquid-encapsulation method and found that all lines shifted versus indium concentration as expected for standard $Ga_{1-x}In_xAs$ pseudobinary compounds.[8] This shows that, even in this rather dilute range of alloy composition, no specific effect associated with the incorporation of In in the bulk material could be found which correlates with the reduction in dislocation density.

In this work, we report for the first time on the low-temperature near-band-gap photoluminescence (PL) measurements of a series of epitaxial GaAs layers, grown by organometallic–vapor-phase epitaxy (OMVPE). The calibrated indium concentrations ranged between 0 and $6.5\times10^{19}$ cm$^{-3}$ (i.e., between 0 and 0.3% with respect to GaAs mole concentration). This is about 1 order of magnitude below the typical compositions investigated in the works of Refs. 6 and 7 and corresponds to a very dilute range. The sample preparation and the experimental details are described in Sec. II, as well as the determination of indium concentration by x-ray diffraction and secondary-ion mass spectroscopy (SIMS). The PL results are presented and discussed in Sec. III, while, in Sec. IV, we analyze the PL intensities versus indium content.

## II. EXPERIMENTAL

### A. Sample preparation

We have grown a series of five GaAs:In layers with various indium concentrations, including an In-free one used as a reference sample. We proceeded by OMVPE on substrates which have been sliced from the same

 

liquid-encapsulated Czochralski (LEC) -grown, semi-insulating, GaAs:Cr wafer (Wacker Chemitronic). All substrates had an EPD value less than 30 000 $cm^{-2}$ and, to avoid perturbations by the well-known inhomogeneities of the ingot along the diameter,[9] every $10\times10$-$mm^2$ piece of substrate has been cut from equidistant areas measured from the center of the wafer. After cleaning in organic solvents and etching 2 min in an $H_2SO_4$:$H_2O_2$:$H_2O$ solution (50 °C), $n$-type GaAs:In layers with 5 $\mu$m thicknesses have been grown at 640 °C by atmospheric pressure OMVPE. Trimethylgallium (TMG), trimethylindium (TMI), and $AsH_3$ have been used as sources for GaAs:In with a $[A^{V}]/[B^{III}]$ mole ratio of 10. The indium concentration was controlled by adjusting the flow of TMI into the reactor. All details of the growth system have been described earlier.[10]

In order to minimize the effect of shallow impurities, and to reveal more distinctly the effect of indium incorporation, no intentional doping was introduced. Although the growth system was carefully cleaned before every series of runs, we expect, besides the well-known OMVPE-process-specific impurity C, residual amounts of contaminations by Se, Zn, and Mg. This is because these elements have been used as dopants in previous series of runs. In order to clean up the system, first a GaAs dummy layer was grown and, afterwards, all layers dedicated to the PL measurements. The details of sequences and growth conditions have been summarized in Table I. Also show in Table I are the electrical properties of the layers as determined by Hall measurements. During the sequence of growth runs a decrease of the free-electron concentration and an increase of the 300 and 77 K mobilities can be observed which is, roughly speaking, independent the indium concentration. This indicates a purification of the growth system from run to run and, hence, a lower compensation in the layers. A closer look, however, shows that run 4 slightly disagrees with the average tendency. This indicates an accidental increase in the number of residual acceptors (carbon?) and should correlate with some differences in PL intensities.

### B. PL measurements

Most PL measurements have been done with samples held at 2 K. They were excited with the 647.1-nm $Kr^+$ laser line, at a power density ranging between 6 and 60 $mW/cm^2$. When necessary a system of gas helium flow allowed the temperature to vary between 2 and 20 K. The emitted light was collected using a cassegrain-type system, dispersed by a 0.5-m grating monochromator and detected by an optical multichannel analyzer using 500 silicon targets in 400 lines. The resolution was 0.1 meV in the spectral range investigated.

### C. Quantitative determination of the indium concentration

A special care was taken to determine quantitatively the indium concentration in our GaAs:In layers. For the highest In concentrations, the lattice constants were determined by using a precision double crystal x-ray diffractometer and the $\langle 115 \rangle$ reflexion of the crystal monochromator. Then the strain-free lattice constant was calculated, assuming the lattice matched to the substrate ($\Delta a_{\parallel}/a_{\text{substrate}}=0$) and a Poisson ratio of 0.29. Finally, by simply applying the Vegard's law, the In concentrations shown in Table I could be calculated. Since, for low In concentrations, the respective x-ray diffraction peaks associated with the substrate and the epilayer could not be resolved, quantitative SIMS measurements have been performed. This was next generalized to determine the relative In concentrations in the different layers and the ratio of $^{113}In$ counts normalized to the $^{75}As$ matrix signal is also given in Table I.

The combination of x-ray and SIMS data ensured reliable results for the In concentration in all samples; and a comparison between the absolute x-ray determination and the relative SIMS data shows good agreement on the samples with high indium concentration. An estimated upper error limit is finally given in Table I.

## III. RESULTS AND DISCUSSION

### A. In-free GaAs

A typical PL spectrum, characteristic of our In-free GaAs reference sample at 2 K is displayed in Fig. 1. Using an excitation fluence of 6 $mW/cm^2$, the bound-exciton bands at 1.51 eV have been found quite similar to those reported in Refs. 11 and 12. In particular, the lines associated with excitons bound to neutral donors ($D^0X$ at 1.5146 eV), ionized donor ($D^+X$ at 1.5139 eV), and neutral acceptor ($A^0X$ at 1.5128 eV), respectively, can be

TABLE I. Sequence of growth runs, Hall measurements data, and indium concentrations [In] in GaAs:In OMVPE layers, as determined by x-ray diffraction and quantitative SIMS measurements. The [In] values in % are listed with respect to GaAs molecular concentration. In the last column, estimated upper error limits are also displayed.

| Growth run | $N_D-N_A$ ($10^{15}$ $cm^{-3}$) | Mobility (Hall meas.) ($cm^2V^{-1}s^{-1}$) 300 K | 77 K | [In] (x-ray diffraction) ($10^{19}$ $cm^{-3}$) | (%) | $^{113}In/^{75}As$ SIMS counts | [In] (combination of x-ray and SIMS data) ($10^{19}$ $cm^{-3}$) | (%) |
|---|---|---|---|---|---|---|---|---|
| 1 | 4.5 | 4350 | 22 330 | Dummy Layer | | | | |
| 6 | 0.9 | 7066 | 51 060 | In-free GaAs | | | | |
| 5 | 0.8 | 7097 | 51 160 | not resolved | | 193 | 0.7 | 0.03±0.01 |
| 4 | 0.5 | 7323 | 17 555 | (0.9) | (0.04) | 320 | 1.1 | 0.05±0.01 |
| 2 | 1.3 | 6778 | 38 520 | 1.90 | 0.086 | 530 | 1.90 | 0.086±0.005 |
| 3 | 1.3 | 7145 | | 6.34 | 0.287 | 1780 | 6.41 | 0.290±0.005 |

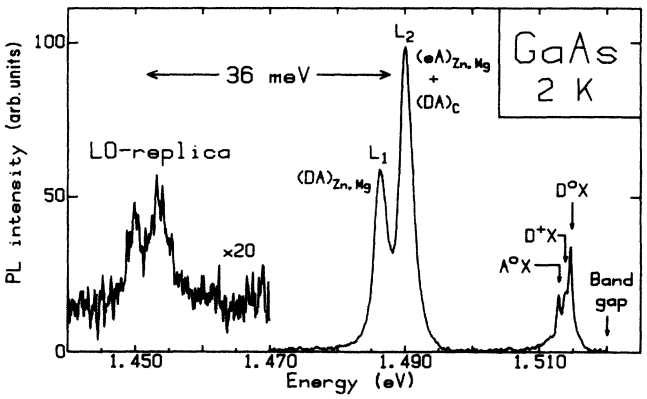


FIG. 1. Photoluminescence spectrum of our In-free GaAs layer (OMVPE growth run 6). Data obtained at 2 K with an excitation power density of 6 mW/cm$^2$. $L_1$ and $L_2$ refer to $(DA)_{Zn,Mg}$ and $(DA)_C$ transitions, respectively.

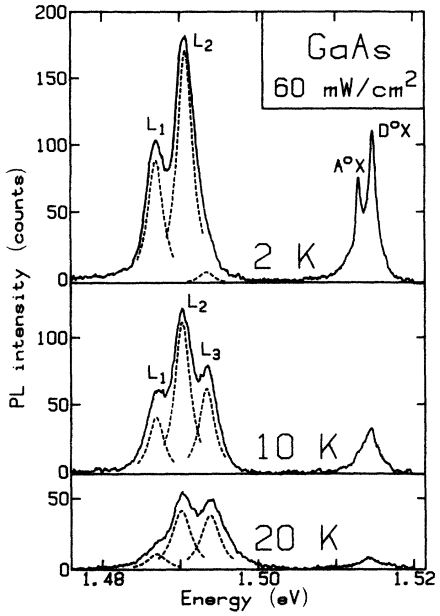


FIG. 2. Temperature dependence (range 2–20 K) of the near-band-edge photoluminescence for our In-free reference layer. The excitation density was 60 mW/cm$^2$. $L_1$, $L_2$, and $L_3$ correspond to $(DA)_{Zn,Mg}$, $(eA)_{Zn,Mg}+(DA)_C$, and $(eA)_C$ transitions, respectively. The different acceptor-related transitions have been fitted according to the simple model discussed in the text.

easily recognized. The PL bands at about 1.49 eV, labeled $L_2$ and $L_1$, respectively, correspond to transitions toward shallow acceptor levels where the excited carriers come from either the conduction band ($eA$ at $\simeq 1.490$ eV) or a shallow donor level ($DA$ at $\simeq 1.486$ eV) (see Refs. 11, 13, and 14 for instance). Lastly the much weaker PL band around 1.45 eV are the one-phonon replica of the $L_1$ and $L_2$ bands at $\simeq 1.49$ eV. Both involve the well-known 36 meV LO phonon of GaAs.

Concerning the two PL bands at 1.490 and 1.486 eV, a point is worth noticing. Both were associated with transitions involving Zn and/or Mg acceptors[13,15] where, in both cases, the impurity substitutes onto a Ga site. A third impurity should also occur in an OMVPE reactor, which behaves like a residual acceptor. This is carbon substituted onto an As site. Since we expect In, introduced as an isoelectronic impurity in GaAs, to reduce the number of Ga vacancies, we expect to find the following.

(i) The magnitude of the recombination lines involving carbon should be independent of the In concentration. (They should be only dependent on our OMVPE reactor and stay fairly constant from sample to sample.)

(ii) The magnitude of the recombination involving zinc and magnesium should decrease.

Recently, Zemon *et al.*[16] have shown that the related Zn-, Mg-, and C-features could be separately revolved in high-purity OMVPE and MBE samples, using low excitation densities and applying a magnetic field. Although the width of the PL lines decreases when decreasing the excitation intensity we could not revolve these specific features because of a too high level of residual acceptors in our samples. We shall come back to this point later.

In order to overpass this problem and get more informations about the specific presence of carbon in our samples, temperature-dependent PL measurements have been performed. The excitation density was 60 mW/cm$^2$ and the temperature ranged between 2 and 20 K. Figure 2 shows the temperature dependence of both the excitonic bands and the $L$ bands. As expected the intensity of $L_1$ decreases while a new line ($L_3$), located at 1.493 eV, appears at 10 K. This new line comes from transitions involving carbon substituted for arsenic ($C_{As}$)[12–14,17] and is initiated via thermal reexcitation of shallow donors above 10 K. The appearance of a C-specific band at higher temperature implies that the $L_2$ band at 1.4901 eV is actually a nonresolved superposition of $(eA)_{Zn,Mg}$ band and transitions between donors and C acceptors $(DA)_C$.

To make this point clear, we have performed a simple calculation. Let $K$ and $(1-K)$ define, the percentage of neutral and ionized donors, respectively; let $S_1$ and $S_3$ define the total PL intensities associated with the two different paths involving Zn or Mg on the one hand, and C on the other hand; we get for lines $L_1$ and $L_3$ the respective intensities:

$$I_1 = KS_1 \quad \text{and} \quad I_3 = (1-K)S_3 \ .$$

This gives for the intensity of the intermediate band $L_2$

$$I_2 = kI_1 + I_3/k \ ,$$

where $k=(1-K)/K$ is the ratio of ionized to neutral donors. We have performed a quantitative comparison, assuming a series of Lorentzian shapes with identical broadening parameters. The results are shown in Fig. 2. This analysis shows that both $(eA)_{Zn,Mg}$ and $(DA)_C$ transitions fairly participate in the $L_2$ line at 10 K, while, at 2 K, mainly carbon-related $DA$ transitions are involved.

### B. GaAs:In

The effect of indium incorporation on both the excitonic structures and the $L$ bands is summarized in Fig. 3. All spectra have been recorded at 2 K with the same sensitivity and the same excitation power density of 6 mw/cm$^2$.

#### *1. Shifts in energy position of the PL lines at 2 K*

Concerning the change in energy position of the bound-exciton lines, we find a shift toward lower energy which correlates well with already reported data for

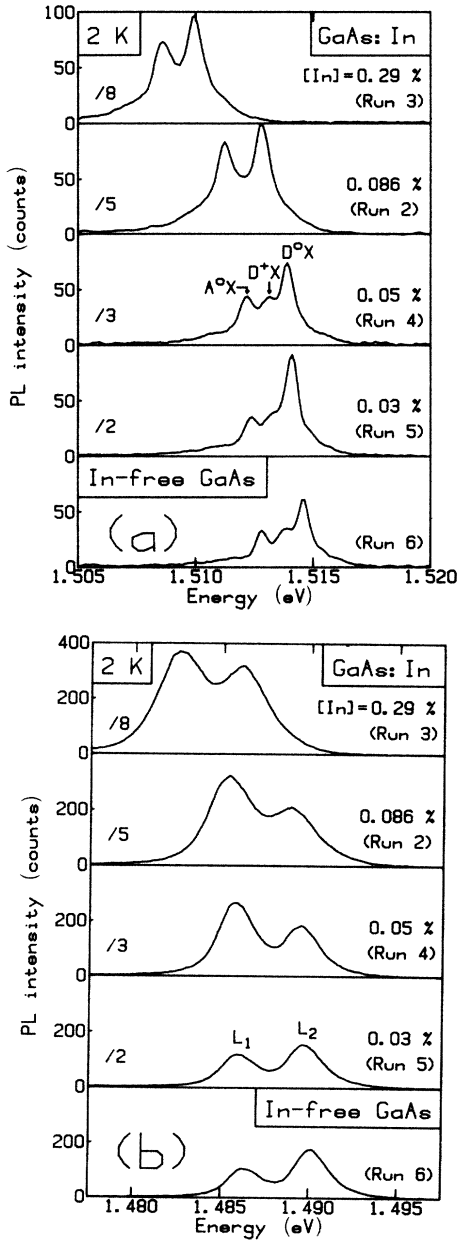


FIG. 3. Composition dependence of the near-band-edge PL features, obtained at 2 K with a constant excitation power density of 6 mW/cm$^2$. (a) $A^0X$ and $D^0X$ bound-exciton lines; (b) acceptor-related recombination lines. $L_1$ and $L_2$ correspond to $(DA)_{Zn,Mg}$ and $(eA)_{Zn,Mg}+(DA)_C$, respectively (see text).

$In_xGa_{1-x}As$ alloys.[8] This demonstrates that, even at concentrations below $10^{19}$ cm$^{-3}$, indium does not act as a substitutional isoelectronic impurity but still fully participates in the composition of a pseudo-binary system. This extends the recent results of Kitahara *et al.*,[6] (i) to epitaxial layers, (ii) to values of $x$ which are lower by 1 order of magnitude.

According to the authors of Ref. 6 the $A^0X$ exciton lines provide the most precise determination of the In concentration while, on the opposite, it was suggested in Ref. 7 to use the shallow acceptor $C_{As}$-related transitions at 1.490–1.493 eV. A check of the different possibilities is shown in Fig. 4. Since, in our OMVPE layers, both the $A^0X$ and $D^0X$ lines were clearly resolved, we believe that they both can be used with the best precision. The nice resolution of these lines, typically 0.5 meV half-width at half maximum [see Fig. 3(a)], would indeed allow an accuracy down to 0.000 3 in indium concentration and the scattering of data in Fig. 4(a) is within this accuracy. To speed up the future determination of In concentration by using this fast, nondestructive, PL technique we have performed a least-mean-squares fit through the experimental data. We find linear dependences $x=-\Delta E/A$, where $\Delta E$ is the energy shift (in eV) of the $A^0X$ and $D^0X$ lines with respect to the In-free sample at 2 K. The values of $A$ are listed in Table II and compared with the shift in free exciton energy, as obtained from Ref. 8 in the limit $x\rightarrow 0$. Considering first $D^0X$, we find a slope parameter $A=1.6216$ eV, which is to be compared with $A=1.5837$ eV in Ref. 8. This very good agreement demonstrates (i) that we are still dealing in GaAs:In with the same solid solution as the one used to lattice-match GaInAs onto InP (in other words there is no significant effect of clustering which would differentiate the two compositional ranges) and (ii) that there is almost no change in exciton binding energy versus indium concentration for this very lightly bound exciton complex. For comparison purposes, we list also the results obtained in the work of Ref. 6. In this case, the experimental slope is slightly different (1.505 eV) but we believe that most of the discrepancy comes from difficulties in quantitatively analyzing indium and in getting good quality, homogeneous, samples.

This is no longer true when comparing on the same sample and, of course, on the same series of experiments, various recombination lines. Coming back to Table II, we find, first, a significant discrepancy between the slope parameters associated with $D^0X$ (1.6216 eV) and $A^0X$ (1.4728 eV). However both are three particles complexes which involve two electrons (or two holes) and one hole (or one electron, respectively) and there is no simple understanding of their respective behavior. Since $D^0X$ behaves like a free exciton, we must conclude that most of the discrepancy comes from the second bound hole which takes part in the neutral ($A^0$) acceptor. Unfortunately, the inherent complexity of a three particles system prevents any simple analysis. What is the part due to the change in acceptor binding energy and/or to the change in correlation effects is, at first glance, difficult to say.

A much simpler situation is encountered when consid-

ering the donor-acceptor recombination lines. At 2 K, we resolved clearly both bands $L_1$ and $L_2$ for the whole series of sample. As already demonstrated for GaAs, they correlate just with $(DA)_{Zn,Mg}$ and $(DA)_C$ transitions, respectively. The same least-squares-fit procedure gives the slope parameters listed in Table II. Opposite to the finding of Ref. 7, we find line-dependent values. First there is a small (but finite) difference between the bound-exciton lines and the donor-acceptor ($D$-$A$) pairs but also between the $D$-$A$ pairs, depending on the chemical species. As a consequence, when using the C-related features at 2 K to probe the indium composition, one should use $x=-\Delta E/A$ with $A=1.4235$ eV instead of 1.6216 or 1.4728 eV for the respective bound-exciton lines. This in an important point to keep in mind, since carbon is the most important impurity in most OMVPE and/or MBE epitaxial layers and as a consequence has already been used to probe the In composition.[7]

TABLE II. Comparison of the slope parameters (eV) obtained in this work with previously published data.

| | This work (2 K) | Ref. 6 (4.2 K) | Ref. 7 (2 K) | Ref. 8 (2 K) |
|---|---|---|---|---|
| $E_g$ | | | | 1.5837 |
| $D^0X$ | 1.6216 | 1.505 | | |
| $A^0X$ | 1.4728 | 1.505 | 1.59 | |
| $(eA)_C$ | | 1.505 | 1.59 | |
| $L_2-(DA)_C$ | 1.4235 | | 1.59 | |
| $L_1-(DA)_{Zn,Mg}$ | 1.3358 | | | |

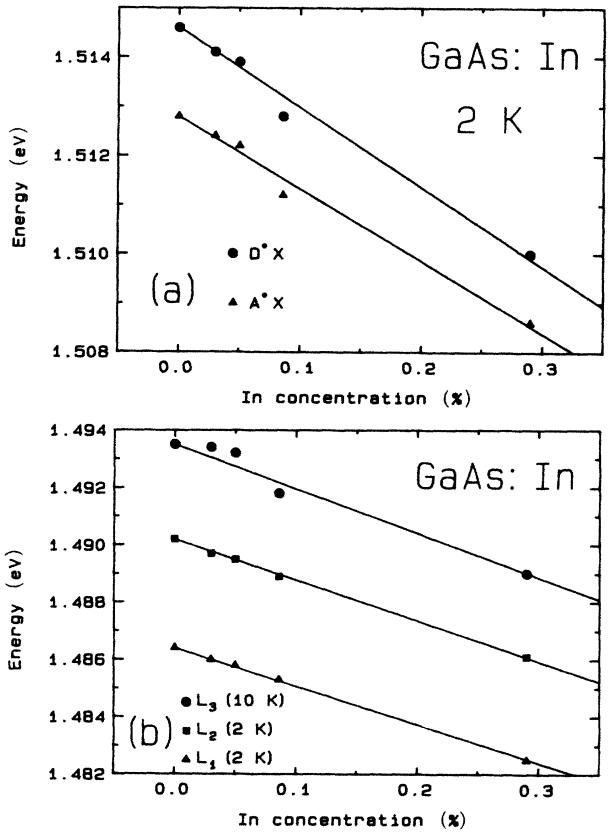


FIG. 4. Energy shift of (a) the two series of $D^0X$ and $A^0X$ transitions resolved at 2 K for the full series of GaAs:In samples. The straight lines correspond to least-mean-squares fits performed through the experimental data and give linear dependences $x(\%)=-\Delta E(\text{eV})/A$. $A$ is line dependent, we find $A=1.6216$ eV for excitons bound to the neutral residual donors and $A=1.4728$ eV for excitons bound to neutral acceptors; (b) same as Fig. 4(a), but for the series of lines $L_1$, $L_2$, and $L_3$. At 2 K, $L_1$ and $L_2$ refer to $(DA)_{Zn,Mg}$ and $(DA)_C$ transitions, respectively. They also give linear slopes $x(\%)=-\Delta E(\text{eV})/A$ where, again, $A$ is line dependent. The corresponding values are listed in Table II. At 10 K, $L_3$ refers to $(eA)_C$ transitions and gives $x(\%)=-\Delta E(\text{eV})/1.548$. Notice the small but finite discrepancy between the slope parameters associated with $L_1$ and $L_2$ transition lines at 2 K (see Table II). This is indicative of site-dependent effects, where the change in binding energy, vs indium content, depends on which sublattice the impurity incorporates. This is discussed in the text.

Since GaAs:In is the prototype of alloys which depart from the virtual-crystal approximation,[18] we have found interesting to check whether the discrepancy between the results concerning Zn/Mg, on the one hand, and C, on the other hand, is only related to chemical effects (differences in core size and atomic energy levels) or correlates also with different substitutional positions. Indeed, Zn and Mg substitute on the cation sites, while C substitutes on the anion site: they might experience different alloy dependences.

To make the calculation as simple as possible, we have used a molecular cluster approximation[19–21] which models the energy levels of the valence band from a cluster of 17 atoms. This allowed the authors of Refs. 19–21 to successfully describe the electronic states of isolated vacancies and substitutional impurities (including C in GaAs). In this work, since we are mainly concerned by the changes in energy associated with (i) the topmost valence band and (ii) the substitutional impurity levels (acceptors), we shall restrict ourselves to the simplest approximation of first-neighbor interactions directed along the bond orbitals (BO). Such a simplified model is not expected to give reliable results for the conduction band, but should significantly deal with (i) the change in energy associated with chemical substitution and (ii) the energy shift associated with alloy composition. Since we did not want to adjust any parameter, all matrix elements have been obtained (i) from existing tables of atomic energy eigenvalues ($E_s$ and $E_p$) in Ref. 22 and (ii) from interaction parameters listed for first-neighbor orbitals in Ref. 23. This gives a density of valence states for GaAs which is displayed in Fig. 5 and compared with (i) the theoretical results of Ref. 19 and (ii) the valence-band x-ray photoemission spectrum.[24] As already said no free parameter enters the calculation and we have only set the zero energy in order that the maximum associated with the upper valence states (our model) fits with the experimental photoemission maximum $P_I$. In both configurations (central Ga or As atom), we obtain a too narrow bandwidth. Indeed the lower valence states lie at about 2 eV above the deeper photoemission band $P_{III}$. Moreover, except

TABLE III. Comparison of slope parameters obtained in this work with the change in acceptor binding energies obtained for Zn, Mg, and C. Working under the VCA, we cannot explain the slight but finite discrepancy experimentally observed in terms of perturbations associated with the different atomic energy values (chemical shifts).

| | Calculation (VCA approximation) | | | Experiment |
|---|---|---|---|---|
| | $dE_V/dx$ | $dA_0/dx$ | $dE_B/dx$ | $dE_B/dx$ |
| | +0.71 | | | |
| C | | +0.61 | −0.10 | −0.16 |
| Zn | | +0.61 | −0.10 | −0.25 |
| Mg | | +0.61 | −0.10 | −0.25 |

for a small shoulder at about 5 eV in the central As configuration, no feature is clearly seen which could correspond to the maximum $P_{II}$. Obviously, such a simple BO approximation, together with a cluster of 17 atoms, cannot be used to account quantitatively for existing x-ray photoemission data. However, since the results of our calculation and the experimental spectrum are in much better agreement in the range of energy close to the first valence band, we can expect from our simple model a rather good description of the upper valence states and the shallow acceptor bound states.

Consider now the solid solution $Ga_{1-x}In_xAs$. We first use the so-called virtual-crystal approximation (VCA), taking linear extrapolation (i) of atomic energy terms between respective eigenvalues for Ga and In atoms and (ii)

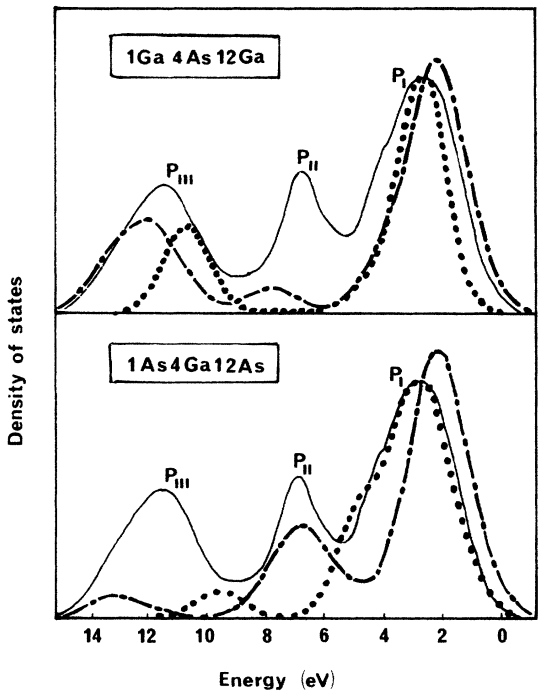


FIG. 5. Density of valence-band states as obtained for GaAs. In full lines are experimental results obtained from Ref. 24. Full-dotted lines give the results of Ref. 19 and the dotted lines have been obtained in this work (bond orbitals approximation). It should be emphasized that no free parameter enters the calculation.

of first-neighbor interactions between GaAs and InAs. In this way, when indium is substituted for gallium, we find a positive energy shift of the topmost valence band:

$$\frac{dE_V}{dx}=0.71 \text{ eV} .$$

Since we cannot expect from our simple calculation any reliable value for the energy shift of the bottom of the conduction band, we shall use, in the remaining part of this work, the experimental value given by the slope parameter of the change in band-gap energy (Ref. 8):

$$\frac{dE_C}{dx}=\frac{dE_g}{dx}+\frac{dE_V}{dx}=-0.87 \text{ eV} ,$$

which is of the same order of magnitude as the positive shift of the valence band that we computed.

The energy of any acceptor state is found by replacing the central atom [in the two cluster configurations: Ga(In)+4As+12Ga(In) or As+4Ga(In)+12As], by Zn/Mg, or C, respectively. We find that all acceptor binding energies decrease, versus indium concentration, with the same slope parameter:

$$\frac{dE_B}{dx}=-0.1 \text{ eV}$$

which is independent of the nature of the impurity and of the site on which it is incorporated. All slope parameters for the topmost valence band, the absolute energy of acceptor states and the change in binding energies for Zn, Mg, and C, are listed in Table III (VCA). Strictly speaking, this shows that our experimental results depart from the simple virtual-crystal approximation and are not associated with chemical (atomic energies) effects. They rely on more subtle effects associated with the first-neighbor interactions at the microscopic scale.

To go even further, we must go beyond the virtual-crystal approximation and discern the two different configurations associated with impurity atoms on Ga(In) and As sites, respectively. Consider first C substituting for As. The four first neighbors are Ga or In, depending on the alloy composition. In this configuration, the virtual-crystal approximation should still hold. Indeed we computed in Table III a slope parameter −0.10 eV, rather close to the experimental value −0.16 eV. On the other hand, for impurities like Zn or Mg substituting on the cation site (Ga and/or In), the four first neighbors are

As whatever is the alloy composition. In this case, for rather low indium concentrations, we can reasonably assume that the impurity-As bond retains its main character (polarity and bond length) whatever is the alloy composition. The changes in binding energy computed in this way are listed in Table IV. The interesting point is that we obtain a much larger decrease in the theoretical binding energy for acceptors like Zn or Mg substituted on the cation sites, as compared with C substituted on As sites. This difference qualitatively agrees with the experimental results and shows that the discrepancies between the different slope parameters of the PL lines in Table II are significant. It is indicative of microscopic behaviors discerning between substitutional impurities on the cation or the anion sites.

### 2. *Temperature dependence*

For the sake of completeness, we have raised the temperature up to 10 K in order to resolve all lines $L_1$ to $L_3$ observed on GaAs. Using a uniform power excitation of 60 mW/cm$^2$, we get the series of poorly resolved spectra displayed in Fig. 6. We cannot resolve the excitonic features any more and the three lines of interest appear only as broad shoulders in the range 1.480–1.495 eV. We have used the line fitting procedure described in Sec. III A to determine the energy positions of the three-recombination lines as a function of indium content. The results appear as dotted lines in Fig. 6. A plot of the corresponding maxima versus indium concentration does not discriminate any site-dependent effect and we only find an average slope parameter which, within experimental uncertainty, agrees with our proceeding values ($A = -1.55 \pm 0.05$ eV).

## IV. CHANGE IN PL INTENSITIES VERSUS INDIUM CONTENT

Coming now to the relative PL intensities of the different samples, we find the following.

(i) The respective intensities of all lines from $(D^0X)$ to $(DA)_{Zn,Mg}$ increase versus indium concentration. This is independent on the growth sequence and can be easily seen from Fig. 3 where scaling factors 2, 3, 5, and 8 have been associated with percent indium concentrations 0.03, 0.05, 0.086, and 0.29, respectively. This overall increase differs completely from the results reported in Ref. 25

TABLE IV. Same as Table III but using a microscopic approach which departs from the VCA (see text). We find that the main difference between C, on the one hand, and Zn/Mg, on the other hand, lies on the different sublattices on which they incorporate. This results in different slope parameters which qualitatively correlate with the experimental data.

| | Calculation (BO approximation) | | Experiment |
|---|---|---|---|
| | $dA_0/dx$ | $dE_B/dx$ | $dE_B/dx$ |
| C | +0.61 | −0.10 | −0.16 |
| Zn | +0.07 | −0.64 | −0.25 |
| Mg | +0.08 | −0.63 | −0.25 |

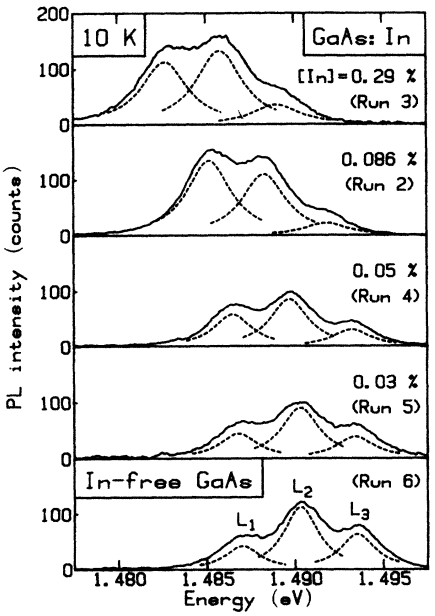


FIG. 6. Composition dependence of the $L_1$, $L_2$, and $L_3$ recombination lines obtained at 10 K with a constant excitation power density of 60 mW/cm$^2$. $L_1$, $L_2$, and $L_3$ correspond to $(DA)_{Zn,Mg}$, $(eA)_{Zn,Mg}+(DA)_C$, and $(eA)_C$ transitions, respectively (see text). They have been fitted according to the simple model discussed in Sec. III A.

and should be viewed as indicating an increase in the average quality of our samples. Whether or not there is an optimum in the In concentration is not well understood. To clarify this point we display in Fig. 7 our experimental results concerning the changes in PL intensity versus alloy composition. All values have been normalized to the In-free reference sample. We find a very rapid

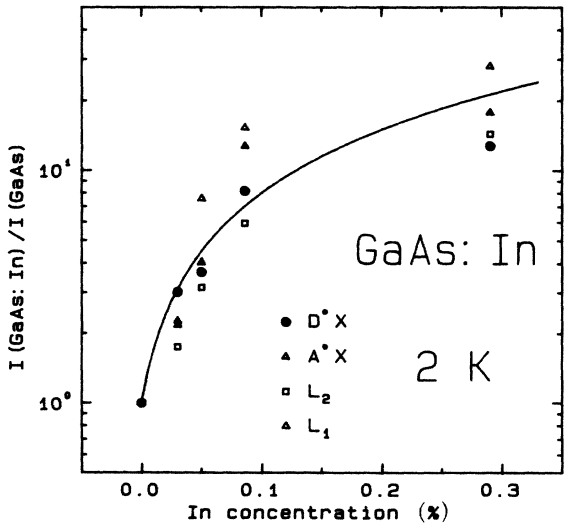


FIG. 7. Changes in PL intensities as a function of indium concentration for $D^0X$, $A^0X$, $L_2$, and $L_1$ lines. All values have been normalized to the In-free reference sample. Notice the rapid jump from $x = 0$ to about 0.1% which next saturates.

jump from $x=0$ to about 0.1% which next saturates. As for as PL intensities are involved, this seems to demonstrate that the best In composition is about 0.1%.

(ii) This increase *does not* correlate with a higher purity of our reactor from run to run. We have indeed observed such a purification effect: it corresponds to the relative intensity of $L_1$ versus $L_2$. Switching from run 2 ($x=0.086\%$) to run 3 ($x=0.29\%$) we find the increase in intensities already noticed (increasing In concentration) but a relative decrease in $L_1$ (Zn,Mg) with respect to $L_2$ (carbon). This is evidence of the purification effect. It continues from run to run, up to run 6 (In-free GaAs). This is shown in Fig. 8 where the concentration of residual impurities is found approximately lower by a factor for run 6 with respect to run 2. (iii) From a close consideration of points (i) and (ii) we must conclude that the low level of PL intensity in pure GaAs (run 6), with respect to In-doped materials, *cannot* come from an effect of purification of the reactor. Moreover, since C incorporates on the As sites, we expect the corresponding line intensity to be independent of the indium concentration. This assumption is supported by the simple fact that, during the growth process, an infinite number of free lattice sites is available at the surface. The presence of a few In atoms on the reacting crystal surface cannot prevent the incorporation of these acceptors introduced via the gas phase. In other words the signal intensity associated with carbon should present a fairly constant level, which is opposite to the experimental findings (see Fig. 3). This shows that, introducing indium, we decrease the path for defect-associated transitions, i.e., we increase the average optical quality of our samples.

One point should be now further investigated. It concerns the nature of the corresponding defects. Since the drastic changes in optical properties in the near-band-gap region correlate only with rather small changes in electrical properties (see Table I), we suggest that in our material the incorporation of In acts primarily on the concentration of hole traps (which lowers the PL on that part of the spectrum) and not on the density of electron traps (which rule the mobility of the carriers in our $n$-type samples).

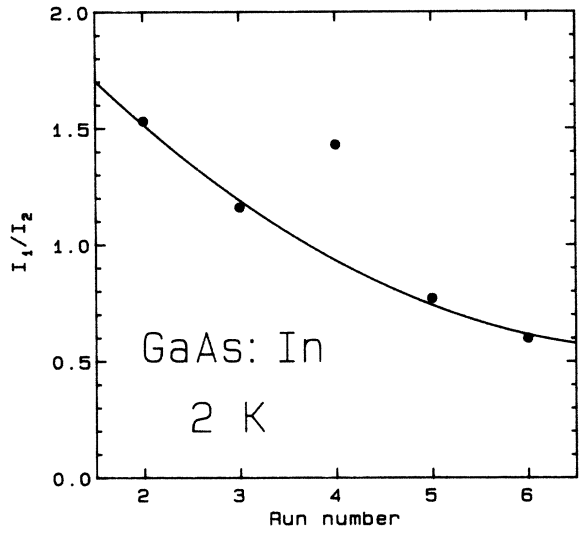


FIG. 8. PL intensity ratio of $L_1$ over $L_2$ lines involving Zn-, and/or Mg- and C-acceptors, respectively, as a function of the run number. The decrease, by a factor of 3, of the concentration in residual impurities (Zn and Mg) corresponds to a purification effect of our reactor from run to run. It prevents the association of the (relatively) poor luminescence intensity of our In-free sample (run 6) with a higher degree of contamination and shows that, incorporating indium, we have indeed closed some nonradiative-recombination path.

## V. CONCLUSION

We have investigated the influence of indium incorporation on the near-band-edge photoluminescences of GaAs. We have found the following.

(i) Even at very low concentration, indium incorporates like a constituent of the solid solution $Ga_{1-x}In_xAs$. We could not find any evidence of clustering between neighboring indium atoms, giving similar structures to the so-called NN pairs in GaP (Ref. 26) or $Te_n$ centers in ZnS and CdS.[27,28] We could neither find evidence for a disorder-related enhancement of the polarization recombination lines, similar to the one reported for II-VI compounds.[29]

(ii) A quantitative analysis of the indium composition can be performed from the shift of the main PL lines. We find that both the $D^0X$ or $A^0X$ on the one hand, and the $DA$ or $eA$ recombination lines, on the other hand, can be used but with different slope parameters. By using a simple model of 17 atoms molecular cluster, we show that the difference between the slope parameters corresponding to the substitutional acceptors (Zn,Mg) and C is indicative of a microscopic behavior discerning between impurities substituting on the cation or the anion site, respectively.

(iii) Versus indium concentration, the intensities of the different PL lines increase. A saturation is reached for $x \approx 0.1\%$.

(iv) To clarify the role of indium, there is a need for investigating the deep traps which exist in our material. Since we believe that, by closing a deep recombination path, indium increases the intensity of the near-band-edge PL lines, further insight into the physics of the deep centers is needed in order to shed more light on the way indium acts in GaAs.

## ACKNOWLEDGMENTS

The authors would like to thank Dr. M. Maier for his contributions of x-ray diffraction and SIMS measurements. J. P. Laurenti deeply thanks the Deutscher Akademischer Austauschdienst for a special support during his visit in the Institute of Semiconductor Electronics (Aachen, Germany). This work was also supported partly by the PROCOPE program.

*Permanent address: Groupe d'Etude des Semiconducteurs, Université des Sciences et Techniques du Languedoc, F-34060 Montpellier Cédex, France.

[1]G. Jacob, M. Duseaux, J. P. Farges, M. M. B. van den Boom, and P. J. Roksnoer, J. Cryst. Growth **61**, 417 (1983).

[2]M. Duseaux and S. Martin, *Semi-Insulating III-V Materials* (Shiva, Kahnee-ta, 1984), p. 118.

[3]H. Beneking, P. Narozny, and N. Emeis, Appl. Phys. Lett. **47**, 828 (1985).

[4]P. Narozny and H. Beneking, Electron. Lett. **21**, 1050 (1985).

[5]H. Schumacher, P. Narozny, Ch. Werres, and H. Beneking, IEEE Electron. Devices Lett. **7**, 26 (1986).

[6]K. Kitahara, K. Kodama, and M. Ozeki, Jpn. J. Appl. Phys., **24**, 1503 (1985).

[7]P. W. Yu, D. C. Walters, and W. C. Mitchel, J. of Appl. Phys. **60**, 3864 (1986).

[8]K. H. Goetz, D. Bimberg, H. Jürgensen, J. Selders, A. V. Solomonov, G. F. Glinskii, and M. Razeghi, J. Appl. Phys. **54**, 4543 (1983).

[9]See, for example, M. Tajima, Appl. Phys. Lett. **46**, 484 (1985).

[10]P. Roentgen and H. Beneking, *Institute of Physics Conference Series* (IOP, Bristol, 1986), Vol. 79, p. 145.

[11]Y. V. Zhilyaev, V. V. Krivolapchuk, A. V. Rodionov, V. V. Rossin, T. V. Rossina, and Y. N. Sveshnikov, Phys. Status Solidi A **89**, K61 (1985).

[12]T. F. Kuech, R. Potemski, and T. I. Chappell, J. Appl. Phys. **58**, 1196 (1985).

[13]D. J. Ashen, P. J. Dean, D. T. J. Hurle, J. B. Mullin, A. M. White, and P. D. Greene, J. Phys. Chem. Solids **36**, 1041 (1975).

[14]D. C. Reynolds, C. W. Litton, E. B. Smith, P. W. Yu, and K. K. Bajaj, Solid State Commun. **42**, 827 (1982).

[15]P. W. Yu, W. M. Theis, and W. Ford, J. Appl. Phys. **57**, 4514 (1985).

[16]S. Zemon, P. Norris, E. S. Koteles, and G. Lambert, J. Appl. Phys. **59**, 2828 (1986).

[17]V. Swaminathan, D. L. van Haren, J. L. Zilko, P. Y. Lu, and N. E. Schumaker, J. Appl. Phys. **57**, 5349 (1985).

[18]J. C. Mikkelsen, Jr. and J. B. Boyce, Phys. Rev. B **28**, 7130 (1983).

[19]A. Fazzio, J. R. Leite, and M. L. De Siqueira, J. Phys. C **12**, 513 (1979).

[20]A. Fazzio, J. R. Leite, and M. L. De Siqueira, J. Phys. C **12**, 3459 (1979).

[21]L. M. R. Scolfaro, R. Pintanel, V. M. S. Gomes, J. R. Leite, and A. S. Chaves, Phys. Rev. B **34**, 7135 (1986).

[22]W. A. Harrison, in *Electronic Structure and the Properties of Solids* (Freeman, San Francisco, 1979), p. 534.

[23]D. J. Chadi and M. L. Cohen, Phys. Status Solidi B **68**, 405 (1975).

[24]L. Ley, R. A. Pollak, F. R. McFeely, S. P. Kowalczyk, and D. A. Shirley, Phys. Rev. B **9**, 600 (1974).

[25]P. K. Bhatacharya, S. Dhar, P. Berger, and F. Y. Juang, Appl. Phys. Lett. **49**, 470 (1986).

[26]See, for instance, B. Gil, J. P. Albert, J. Camassel, H. Mathieu, and C. Benoit a la Guillaume, Phys. Rev. B **33**, 2701 (1986).

[27]K. P. Tchakpele, J. P. Albert, and C. Gout, J. Cryst. Growth **72**, 151 (1985).

[28]W. Heimbrodt and O. Goede, Phys. Status Solidi B **135**, 2701 (1986).

[29]H. Mariette, Y. Marfaing, and J. Camassel, in *Proceedings of the 18th International Conference on the Physics of Semiconductors, Stockholm, 1986,* edited by O. Engstrom (World Scientific, Singapore, 1987), p. 1405.